Navigation Accuracy Category-Position Models and Estimate Position Uncertainty Calculations for TIS-B System

Zhang Qingzhu[a],*, Zhang Jun[a], Zhu Yanbo[b], Liu Wei[b]

[a]*School of Electronics and Information Engineering, Beijing University of Aeronautics and Astronautics, Beijing 100191, China*

[b]*Aviation Data Communication Corporation, Beijing 100083, China*

Abstract

Navigation accuracy category-position (NACp) is an important parameter for system accuracy of traffic information service-broadcast (TIS-B), which is determined by estimate position uncertainty (EPU). Centered about the problems that the existing EPU calculation based on noise measurement is low in accuracy and unfit for describing uncorrected biases in target reports, this article analyses the traditional NACp model, and uses the least square estimation (LSE) in EPU calculation. Furthermore, it proposes an extended NACp model, which considers both noise and biases and acquires EPU estimation with the help of approximate multiplex Taylor expression. Analysis and simulation show that the proposed method not only leads to significant improvement of the accuracy of EPU calculation, but is fit for EPU calculation with tracking biases in TIS-B system as well. As such it can find application in practice to depict different kinds of error models in TIS-B system.

Keywords: error analysis; model; estimation; surveillance radar; traffic information service-broadcast

1. Introduction

Automatic dependent surveillance-broadcast (ADS-B) is the main technology recommended by international civil aviation organization (ICAO) in the next generation of air traffic management (ATM) to replace the existing secondary surveillance radar (SSR). In the interim, the traffic information service-broadcast (TIS-B) is provided as an important surveillance service. It transforms the traffic information from the SSRs outside ADS-B areas into the navigation data format, and delivers it to the ADS-B-equipped aircraft or surface vehicles in ADS-B areas so as to allow ADS-B users to acquire the information about the real-time state (position, velocity and altitude, etc.) of surrounding targets without ADS-B attached, thus supporting the applications of aircraft separation assurance (ASA)[1].

Some of the main ASA applications can be listed as follows[1]:

(1) Enhanced visual acquisition (EVAcq);

(2) Conflict detection (CD);

(3) Airport surface situational awareness (ASSA);

(4) Final approach runway occupancy awareness (FAROA);

(5) Enhanced visual approach (EVApp).

ADS-B minimum aviation system performance standards require that ADS-B and TIS-B systems should provide the parameter pertinent to its position accuracy according to navigation accuracy category-position (NACp), which determines whether the reported position attains the acceptable level for ASA applications[2]. NACp level is determined by estimate position uncertainty (EPU). EPU is an accuracy bound on horizontal position, which is defined as the radius of a circle with its center on the reported position, as such the probability of the actual position lying within the circle is 95%. The definition of vertical EPU (VEPU) is the same as that of EPU[2]. Table 1 lists NACp levels and their matched ASA applications[1].

Table 1 NACp levels matched with ASA applications

NACp	95% horizontal and vertical accuracy bounds (EPU and VEPU)	ASA applications
0	EPU ≥ 18 520 m	none
1	EPU < 18 520 m	none
2	EPU < 7 408 m	none
3	EPU < 3 704 m	none
4	EPU < 1 852 m	none

*Corresponding author. Tel.: +86-10-82317847-6312.

E-mail address: zhangqz_buaa@163.com

NACp	95% Horizontal and vertical accuracy bounds (EPU and VEPU)	ASA applications
		Continued
5	EPU < 1 111.2 m	EVAcq, CD
6	EPU < 370.4 m	EVAcq, CD
7	EPU < 185.2 m	EVAcq, CD, EVApp
8	EPU < 92.6 m	EVAcp, CD, EVApp
9	EPU < 30 m, VEPU < 45 m	EVAcq, CD, ASSA, FAROA, EVApp
10	EPU < 10 m, VEPU < 15 m	EVAcq, CD, ASSA, FAROA, EVApp
11	EPU < 3 m, VEPU < 4 m	EVAcq, CD, ASSA, FAROA, EVApp

As a key in encoding NACp, EPU can be obtained by calculating with onboard ADS-B equipments[2-3].

In spite of the same definitions of NACp and EPU used by both ADS-B and TIS-B, they differ in that ADS-B data come from global position system (GPS) constellation orientation, while TIS-B data from SSR scan, as such GPS's error characteristics are always considered as an isotropic and zero-mean model, while SSR's an anisotropic and non-zero-mean model[4-6]. Therefore, the EPU calculation (i.e., NACp encodes) for ADS-B can not be applied to TIS-B[1, 2, 7-8].

In Ref.[7], R. Chamlou, et al. have proposed an EPU method for TIS-B. Less accurate in determining NACp levels, the method takes into account noise in target reports rather than uncorrected biases, which restricts its application in practice. Therefore, based on the error characteristics of TIS-B data sources, this article suggests a way to improve the accuracy of the existing method an order of magnitude by providing the least squares estimation (LSE) for EPU calculation in the traditional NACp model. Furthermore, for the tracks inclusive of both noise and biases, this article proposes an extended error model of NACp and demonstrates using approximate multiplex Taylor expression to calculate EPU. Analysis and simulation results show that the proposed method to deal with different kinds of track errors in TIS-B system not only can bring about significant improvements of the accuracy of EPU calculation for tracking noise, but also is fit for EPU calculation for both noise and biases.

2. Traditional NACp Model and EPU Calculation

2.1. Traditional NACp model

The distribution of TIS-B system uncertainties can be viewed as a horizontal Gaussian ellipse with its center on a reported position if taking only the tracking noise into consideration[1,7].

$Z \in \mathbf{R}^{2 \times 1}$ denotes the position random errors about the target measurement (μ_x, μ_y) in the *X-Y* plane coordinates, that is

$$Z = [x - \mu_x \quad y - \mu_y]^{\mathrm{T}} \tag{1}$$

$V \in \mathbf{R}^{2 \times 2}$ denotes the error covariance matrix for the target measurement in the *X-Y* plane coordinates, that

is

$$V = \begin{bmatrix} \mathrm{Var}(x) & \mathrm{Cov}(x, y) \\ \mathrm{Cov}(x, y) & \mathrm{Var}(y) \end{bmatrix} = \begin{bmatrix} \sigma_x^2 & \rho\sigma_{xy} \\ \rho\sigma_{xy} & \sigma_y^2 \end{bmatrix}$$

where

$$\rho = \frac{\sigma_{xy}^2}{\sigma_x \sigma_y} \tag{2}$$

The joint Gaussian probability distribution function (PDF) of position variables *x* and *y* is

$$f(x, y) = \frac{1}{2\pi |V|^{1/2}} \exp(-\frac{1}{2} Z^{\mathrm{T}} V^{-1} Z) \tag{3}$$

Eq.(3) is contingent on V, and V can be computed in a Kalman-based estimator[7-9].

The major and minor axes of the 1-σ horizontal Gaussian ellipse can be calculated as follows[7]:

$$\begin{aligned} \mathrm{axis_{major}} &= \max\left(+\sqrt{\lambda_1}, +\sqrt{\lambda_2}\right) \\ \mathrm{axis_{minor}} &= \min\left(+\sqrt{\lambda_1}, +\sqrt{\lambda_2}\right) \end{aligned} \tag{4}$$

where

$$\lambda_{1,2} = \frac{\left(\sigma_x^2 + \sigma_y^2\right) \pm \sqrt{\left(\sigma_x^2 - \sigma_y^2\right)^2 + 4\sigma_{xy}^4}}{2} \tag{5}$$

The angle between *X*-axis and the major axis of the ellipse is[7]

$$\theta = \frac{1}{2}\arctan\left(\frac{2\rho\sigma_x\sigma_y}{\sigma_x^2 - \sigma_y^2}\right) \tag{6}$$

Angles θ may be different in the given covariance matrices (i.e., different ellipses) from different measurements. It seems more convenient for computation to transform *X-Y* coordinates so that the error ellipses turn orthogonal, where $\rho = 0$, $\theta = 0$[7].

Then V becomes

$$V_{\mathrm{m}} = \begin{bmatrix} \sigma_{\mathrm{m}x}^2 & 0 \\ 0 & \sigma_{\mathrm{m}y}^2 \end{bmatrix}$$

where

$$\begin{aligned} \sigma_{\mathrm{m}x} &= \mathrm{axis_{minor}} \\ \sigma_{\mathrm{m}y} &= \mathrm{axis_{major}} \end{aligned} \tag{7}$$

The PDF becomes

$$f_{\mathrm{m}}(x, y) = \frac{1}{2\pi |V_{\mathrm{m}}|^{1/2}} \exp(-\frac{1}{2} Z^{\mathrm{T}} V_{\mathrm{m}}^{-1} Z) \tag{8}$$

Based on Eqs.(4)-(6), V_{m} can be obtained through real-time computation for V in every measurement. This article uses above-mentioned transformed coordinates in the following discussion.

NACp model can be defined as an integration of the joint Gaussian PDF within a plane circle with its center on the reported position[1,7-8] (see Fig.1(a)). It can be expressed by Eq.(9) below. When the circle radius
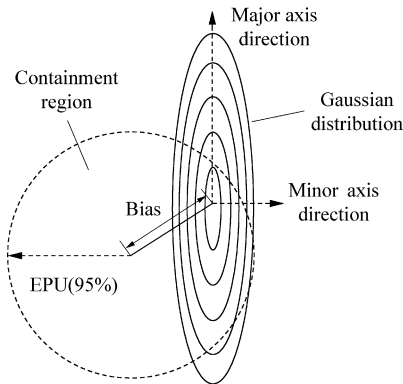
is equal to the value of EPU, the probability (i.e. the integration result) is 0.95.

$$P = \iint_S \frac{1}{2\pi\sigma_{mx}\sigma_{my}} \exp\left[-\frac{1}{2}(\frac{x^2}{\sigma_{mx}^2}+\frac{y^2}{\sigma_{my}^2})\right] dxdy \quad (9)$$

Thus EPU value is determined by V_m, i.e. σ_{mx} and σ_{my}.
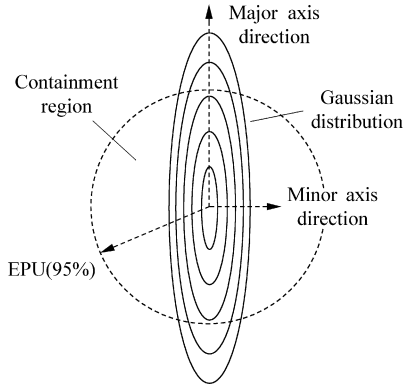
(a) Traditional NACp model for random errors

(b) Extended NACp model considering biases

Fig.1　Two error models for EPU.

2.2. Methods of EPU calculation

Let the radius be $k\sigma_{my}$, in which k is a variable, so the radius depends on k.

Then[7]

$$S : (\frac{x}{k\sigma_{my}})^2 + (\frac{y}{k\sigma_{my}})^2 \le 1 \quad (10)$$

By transforming Eqs.(9)-(10), is acquired P only determined by k and σ_{my}/σ_{mx}. Thus the calculation of EPU is tantamount to the calculation of k when P is 0.95, i.e. the calculation of $k_{0.95}$.

Since no analytical solution can be obtained when integrating Eqs.(9)-(10) to find a closed form, only the numerical integration should be resorted to[7-8]. A method of estimating $k_{0.95}$ is introduced as follows[7]:

$$k_{0.95} = \frac{0.485\,2}{ratio^3} + 1.962\,5$$

where

$$ratio = \sigma_{my}/\sigma_{mx} \quad (11)$$

This article puts forward a revised method to compute $k_{0.95}$ to gain more accurate results. Here let the containment radius equal $k\sigma_{my}$, and σ_{mx} be 1 when σ_{my} increases from 1 to 12. The result which fits with LSE is a third order polynomial as follows

$$\begin{aligned} k_{0.95} = &0.427\,734\,83(\sigma_{mx}/\sigma_{my})^3 + \\ &0.029\,121\,21(\sigma_{mx}/\sigma_{my})^2 + \\ &0.037\,938\,45(\sigma_{mx}/\sigma_{my}) + \\ &1.958\,073\,21 \end{aligned} \quad (12)$$

Then EPU with the value of $k_{0.95}\sigma_{my}$ can be computed.

As a result of verification, Fig.2 illustrates the actual containment probabilities of the radius $k_{0.95}\sigma_{my}$ (i.e. EPU) with respect to σ_{my}/σ_{mx}, in which $k_{0.95}$ is derived from both Eq.(11) and Eq.(12). Table 2 lists the main parameters, with which could be compared the calculation performances between the two above-introduced methods.

From Fig.2 and Table 2, it is obvious that the results calculated with Eq.(12) is better than with Eq.(11) in most cases.

Table 2　Parameters comparison between two methods

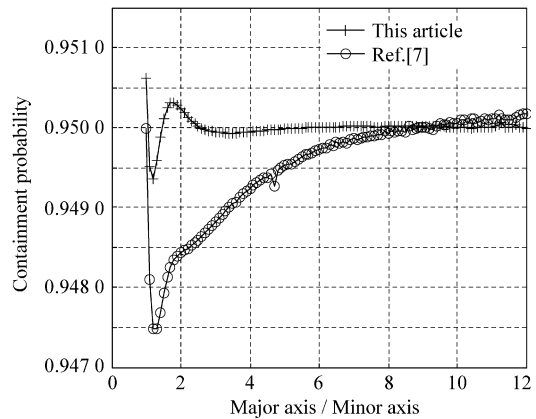| Method	Mean	Variance	Extremum
Ref.[7]	0.949 517 585	$4.398\,371\,6\times10^{-7}$	Max=0.950 21 Min=0.947 49
This article	0.950 002 622	$1.609\,139\,1\times10^{-8}$	Max=0.950 62 Min=0.949 37

Fig.2　Containment probabilities of estimated EPU.

3. Extended NACp Model and EPU Calculation

3.1. Extended NACp model

For some TIS-B tracks of which the biases must not be ignored, the EPU containment radius should take into account both the measured noise and the uncorrected biases. Defined as an offset between the target

measurement report and the aircraft reference point by ADS-B[2], the uncorrected biases are not applicable to TIS-B system, for their data stem from SSR. Actually, the biases in TIS-B system mainly include the inaccuracy of sensors' measurements and the arithmetic transformation as well as the tracking lags due to the target maneuver that may make the trackers' filtered states fall behind the target's true position[6,8].

The presence of biases will enlarge the EPU containment radius and degrade NACp levels, which causes the needs for improving the traditional NACp model. Therefore, this article proposes an extended NACp model (see Fig.1(b)).

In the extended NACP model, $\boldsymbol{D}$ is a 2×1 vector of the integrated biases in the *X-Y* plane coordinates, where $\boldsymbol{D} = [d_x \quad d_y]^T$. Thus the absolute value of $\boldsymbol{D}$ can be computed by the norm L2:

$$\|\boldsymbol{D}\|_2 = \sqrt{d_x^2 + d_y^2} \tag{13}$$

Then Eq.(3) becomes

$$f(x,y) = \frac{1}{2\pi|\boldsymbol{V}|^{1/2}} \exp\left[-\frac{1}{2}(\boldsymbol{Z}-\boldsymbol{D})^T \boldsymbol{V}^{-1}(\boldsymbol{Z}-\boldsymbol{D})\right] \tag{14}$$

In order to adapt the reference frame to the coordinates for which the error ellipses are orthogonal, a coordinates mapping is required for $\boldsymbol{D}$. The transformation is performed as follows

$$\boldsymbol{D}_{\mathrm{m}} = \begin{bmatrix} d_{\mathrm{m}x} & d_{\mathrm{m}y} \end{bmatrix}^T = \begin{bmatrix} \|\boldsymbol{D}\|_2 \cos\alpha & \|\boldsymbol{D}\|_2 \sin\alpha \end{bmatrix}^T$$

where

$$\alpha = \arccos\left(d_x / \|\boldsymbol{D}\|_2\right) - \theta \tag{15}$$

θ can be derived from Eq.(6).

By replacing $\boldsymbol{D}$ with $\boldsymbol{D}_{\mathrm{m}}$, and letting the containment radius remain $k\sigma_{\mathrm{m}y}$, the extended NACp model with the biases considered can be expressed as follows:

$$P_{\mathrm{m}} = \iint_S \frac{1}{2\pi\sigma_{\mathrm{m}x}\sigma_{\mathrm{m}y}} \cdot$$

$$\exp\left\{-\frac{1}{2}\left[\frac{(x-d_{\mathrm{m}x})^2}{\sigma_{\mathrm{m}x}^2} + \frac{(y-d_{\mathrm{m}y})^2}{\sigma_{\mathrm{m}y}^2}\right]\right\} \mathrm{d}x\mathrm{d}y \tag{16}$$

where S is determined by Eq.(10), and P_{m} is the true position containment probability within the dotted-line-outlined circle shown in the extended NACp model (see Fig.1(b)).

3.2. EPU calculation of extended NACp model

A transformation of Eq.(16) is needed before calculation of EPU. Let

$$\left.\begin{array}{l} u = \dfrac{x-d_{\mathrm{m}x}}{\sigma_{\mathrm{m}x}} \\[2mm] v = \dfrac{y-d_{\mathrm{m}y}}{\sigma_{\mathrm{m}y}} \end{array}\right\} \tag{17}$$

then Eq.(16) becomes

$$P_{\mathrm{m}} = \iint_S \frac{1}{2\pi} \exp(-\frac{u^2+v^2}{2})\mathrm{d}u\mathrm{d}v \tag{18}$$

where

$$S: (\frac{\sigma_{\mathrm{m}x}u + d_{\mathrm{m}x}}{\sigma_{\mathrm{m}y}})^2 + (\frac{\sigma_{\mathrm{m}y}v + d_{\mathrm{m}y}}{\sigma_{\mathrm{m}y}})^2 \le k^2 \tag{19}$$

Eq.(19) is equivalent to the following expression

$$S: (\frac{u + d_{\mathrm{m}x}/\sigma_{\mathrm{m}x}}{\sigma_{\mathrm{m}y}/\sigma_{\mathrm{m}x}})^2 + (v + \frac{d_{\mathrm{m}y}}{\sigma_{\mathrm{m}y}})^2 \le k^2 \tag{20}$$

Similarly, the value of EPU can be computed through $k_{0.95}\sigma_{\mathrm{m}y}$ when P_{m} is equal to 0.95. From Eqs.(18)-(20), it is understood that $k_{0.95}$ is determined through $\sigma_{\mathrm{m}y}/\sigma_{\mathrm{m}x}$, $d_{\mathrm{m}x}/\sigma_{\mathrm{m}x}$ and $d_{\mathrm{m}y}/\sigma_{\mathrm{m}y}$. Let $k_1 = \sigma_{\mathrm{m}y}/\sigma_{\mathrm{m}x}$, $k_2 = d_{\mathrm{m}x}/\sigma_{\mathrm{m}x}$, and $k_3 = d_{\mathrm{m}y}/\sigma_{\mathrm{m}y}$. Then $k_{0.95}$ can be regarded as a function with the variables k_1, k_2, k_3

$$k_{0.95} = h(k_1, k_2, k_3) \tag{21}$$

where h can be acquired by fitting the measured k_1, k_2, k_3 and the corresponding measured value of $k_{0.95}$.

Due to the lack of an existing approved expression of h, this article uses Taylor formula to derive an approaching expression of h.

Given $\sigma_{\mathrm{m}x} = 1$, $k_1 = \sigma_{\mathrm{m}y}/\sigma_{\mathrm{m}x} \in [1, +\infty)$, and $k_2, k_3 \in [0, +\infty)$, then the Taylor expression of h beyond the point $(1, 0, 0)$ is

$$k_{0.95} = h(k_1, k_2, k_3) = h(1, 0, 0) +$$

$$\sum_{i=1}^n \frac{1}{i!}\left(k_1\frac{\partial}{\partial k_1} + k_2\frac{\partial}{\partial k_2} + k_3\frac{\partial}{\partial k_3}\right)^i h(1,0,0) + R_n \tag{22}$$

where R_n is the Lagrange remainder.

To compute the initial value of h, i.e. $h(1, 0, 0)$, let $k_1 = 1$, $k_2 = 0$, and $k_3 = 0$ and insert them into Eq.(18) and Eq.(20), P_{m} can be obtained as

$$P_{\mathrm{m}} = \iint_{S:u^2+v^2 \le k^2} \frac{1}{2\pi} \exp(-\frac{u^2+v^2}{2})\mathrm{d}u\mathrm{d}v \tag{23}$$

From which can be deducted the result of $k_{0.95} = 2.447\,7$, i.e. $h(1, 0, 0) = 2.447\,7$[7].

Then, let h be the objective function and determine the estimated order and undetermined coefficients of the polynomial by fitting the measured values with the nonlinear optimization method.

Eq.(22) has three variables. An order n upwards of 3 will complicate either expansion or computation of Eq.(22). Thus this article abandons Eq.(22) and, instead, proposes a simplified conservative method.

3.3. Conservative estimation method of EPU

According to the characteristics of plane Gaussian ellipse (see Fig.2), the gradient of Gaussian probability density is the greatest in the minor axis direction, and the smallest in the major axis. While given the parameters $\|\boldsymbol{D}\|_2$, $\sigma_{\mathrm{m}x}$ and $\sigma_{\mathrm{m}y}$, let t be the angle between

the vector $\boldsymbol{D}_\mathrm{m}$ and the ellipse minor axis.

When t equals $\pi/2$, $\boldsymbol{D}_\mathrm{m}$ and the major axis of the 1-σ plane Gaussian ellipse are located at the same line. Therefore the containment radius is maximum when containment probability is determinate because the gradient of Gaussian probability density is the smallest, i.e. the distribution is the most sparse. This makes $k_{0.95}$ reach the maximum. In contrast, when t equals zero, with $\boldsymbol{D}_\mathrm{m}$ and the minor axis of the ellipse located at the same line, the containment radius is the minimum when containment probability is determinate because the gradient is the greatest, i.e. the distribution is the densest. This makes $k_{0.95}$ reach the minimum. Fig.3 shows the simulation results as the source of the above conclusions with a set of given parameters.
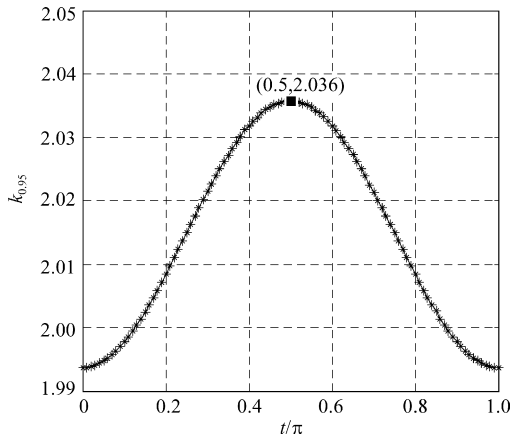

Fig.3 Approximation of $k_{0.95}$ as the function of t ($\sigma_{\mathrm{m}y}/\sigma_{\mathrm{m}x}=4$, $\|\boldsymbol{D}\|_2=1$).

This article proposes an algorithm for conservative estimation of $k_{0.95}$. Suppose that $\boldsymbol{D}_\mathrm{m}$ and the major axis of the ellipse are always located at the same line, i.e. t always equals $\pi/2$, then calculating the maximized $k_{0.95}$.

The conservative estimation will be more than the true value of $k_{0.95}$, because t is not regularly equal to $\pi/2$. From the above-cited research, the error between the maximum of $k_{0.95}$ and the true value takes place when the true value of t equals zero. Fig.4 illustrates
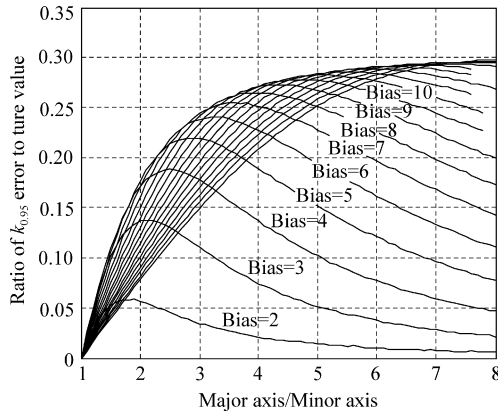

Fig.4 Ratio of $k_{0.95}$ error to true value.

the variation of the ratio of $k_{0.95}$ error to true value

against $\|\boldsymbol{D}\|_2$ and $\sigma_{\mathrm{m}y}/\sigma_{\mathrm{m}x}$. The maximum of the ratio is close to 30%. Thus if the bias can be controlled to a low level, the conservative estimate method of maximized $k_{0.95}$ will gain a much higher accuracy.

The algorithm for conservative estimation of $k_{0.95}$ will be introduced as following discussions.

Let

$$\boldsymbol{D}_\mathrm{c} = \begin{bmatrix} 0 & \|\boldsymbol{D}\|_2 \end{bmatrix}^\mathrm{T} \qquad (24)$$

Replacing $\boldsymbol{D}_\mathrm{m}$ by $\boldsymbol{D}_\mathrm{c}$ in Eq.(16), can be obtained

$$P_\mathrm{m} = \iint_S \frac{1}{2\pi}\exp(-\frac{u^2+v^2}{2})\mathrm{d}u\,\mathrm{d}v \qquad (25)$$

where

$$S:(\frac{u}{\sigma_{\mathrm{m}y}/\sigma_{\mathrm{m}x}})^2 + (v+\frac{\|\boldsymbol{D}\|_2}{\sigma_{\mathrm{m}y}})^2 \le k^2 \qquad (26)$$

Let

$$\left.\begin{array}{l} k_1 = \sigma_{\mathrm{m}y}/\sigma_{\mathrm{m}x} \\ k_2 = \|\boldsymbol{D}\|_2/\sigma_{\mathrm{m}y} \end{array}\right\} \qquad (27)$$

Then $k_{0.95}$ can be converted into a function with the variables k_1 and k_2 as follows

$$k_{0.95} = h(k_1,k_2,0) = g(k_1,k_2) \qquad (28)$$

where g can be fitted by the measured k_1, k_2, and the corresponding measured $k_{0.95}$.

Function g can also be solved with the approaching Taylor formula

$$k_{0.95} = g(k_1,k_2) = g(1,0) +$$
$$\sum_{i=1}^n \frac{1}{i!}\left(k_1\frac{\partial}{\partial k_1} + k_2\frac{\partial}{\partial k_2}\right)^i g(1,0) + R_n \qquad (29)$$

It is obvious that the initial value $g(1,0)$ is equal to $h(1,0,0)$ with a value of 2.447 7. By fitting the measured data with the Levenberg-Marquardt (L-M) method[10], it can be found that the polynomial will satisfy the requirements for application when the order is 4. The objective function of Eq.(29) is equivalent to

$$k_{0.95} = g(k_1,k_2) = c_1 k_1^4 + c_2 k_2^4 + c_{12}k_1 k_2^3 +$$
$$c_{21}k_2 k_1^3 + c_{22}k_1^2 k_2^2 + b_1 k_1^3 + b_2 k_2^3 +$$
$$b_{12}k_1 k_2^2 + b_{21}k_2 k_1^2 + a_{11}k_1^2 + a_{22}k_2^2 +$$
$$a_{12}k_1 k_2 + a_1 k_1 + a_2 k_2 + a_0 \qquad (30)$$

Table 3 lists the estimated coefficients of the polynomial Eq.(30) and Table 4 the performance of the nonlinear optimization.

Table 3 Estimated coefficients of the polynomial

Coefficient	Value	Coefficient	Value
a_0	2.600 569 286 654 49	a_1	−0.573 836 699 661 81
a_2	0.566 574 275 296 113	a_{11}	0.155 408 735 510 93
a_{22}	0.104 934 151 039 261	a_{12}	0.122 698 550 813 67
b_1	−0.017 579 247 214 56	b_2	−0.011 803 417 142 94
b_{12}	−0.011 576 154 514 826	b_{21}	−0.026 359 451 302 24
c_1	0.000 712 756 469 003	c_2	0.000 538 588 234 39
c_{21}	0.001 400 677 373 440	c_{12}	−0.000 192 485 164 36
c_{22}	0.002 891 222 445 252		

Table 4　Performance of the optimization for $k_{0.95}$

RMSE	0.031 117 32	SSE	3.955 453 98
R	0.999 935 05	DC	0.999 870 10
Chi-Square	0.754 273 24	F-Statistic	31 427 426.302 216

Then EPU value through $k_{0.95}\,\sigma_{my}$ can be computed.

Fig.5 illustrates the actual containment probabilities simulation results of the EPU radius, in which $k_{0.95}$ is determined with Eq.(30). In it, the maximum probability is 0.991 8, the minimum 0.904 1, the mean 0.953 2, the standard deviation 0.0447 1 and the average absolute deviation 0.002 45. The probability rises or falls unexpectedly sometimes because the method Eq.(30) is based on fitting the measurements that involve all elements of estimation.
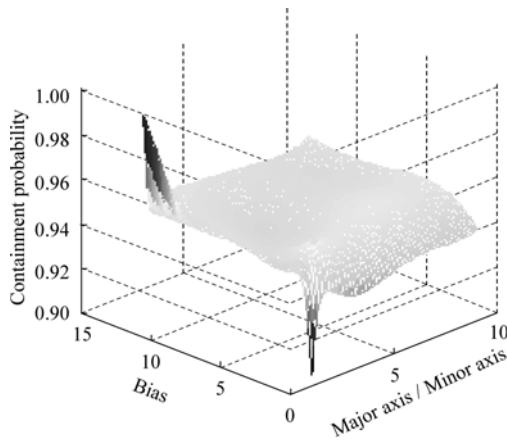
Fig.5　Containment probabilities of EPU radius.

The following section will introduce a method to modify Eq.(30) to attain much higher accuracy.

3.4. Improved method of EPU computation

Based on the characteristics shown in Fig.5, assuming k_m the supposed value of $k_{0.95}$ after modification, and Δk an additive term, then modified EPU will be determined as $k_m\sigma_{my}$, where k_m can be computed from

$$k_m = k_{0.95} + \Delta k . \tag{31}$$

$k_{0.95}$ can also be determined with Eq.(30).

When σ_{my}/σ_{mx} (i.e. k_1) is equal to 1, subtract every measured $k_{0.95}$ and corresponding $k_{0.95}$ from Eq.(30). Fig.6 shows the results in the form of a curve made of "+" symbols.

From Fig.6, it is observed that the beginning and the ending sects of the measurements fall sharply, while the middle remains even but vibrating. This suggests that the curve, through approximate fitting, can be expressed by

$$A(k_1=1,k_2) = p_1 m_1^{t_1 k_2 + n_1} + p_2 m_2^{t_2 k_2 + n_2} + p_3 \sin(t_3 k_2 + n_3) + p_4 \tag{32}$$

with the initial value of k_m is 2.447 7.

Table 5 lists the L-M estimation parameters of Eq.(32) and Table 6 the performance results. Fig.6 shows the better effects attained by the approximation of Eq.(32).
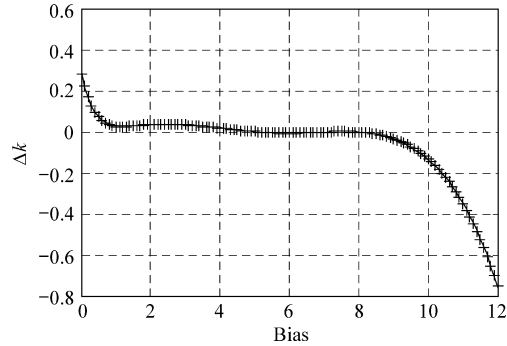
Fig.6　Measured data and approximation of Δk.

Table 5　Optimization parameters of Eq.(32)

Parameter	Value	Parameter	Value
p_1	−0.030 966 195 358	p_2	0.015 429 446 566
p_3	−0.019 609 765 414	p_4	0.017 554 749 966
m_1	1.504 698 416 038	m_2	0.857 218 383 744
n_1	−15.327 498 747 79	n_2	−19.057 584 046 3
n_3	20.790 894 634 951	t_1	1.931 476 913 943
t_2	18.999 255 849 66	t_3	1.042 017 626 312

Table 6　Performance of the Optimization for Eq.(32)

RMSE	0.003 460 88	SSE	0.001 449 300 5
R	0.999 805 96	DC	0.999 611 960 7
Chi-Square	0.020 159 05	F-Statistic	306 550.972 33

Moreover, close scrutiny of Fig.5 discloses that the containment probabilities drop to about 0.95 with the ratio of major axis and minor axis, k_1, increasing. For simplicity, is supposed the ensuing expression:

$$B(k_1) = 1/\exp(k_1 - 1) \tag{33}$$

Thus, by associating Eq.(32) with Eq.(33), Δk can be expressed as

$$\Delta k = B(k_1) \times A(k_1=1,k_2) = [1/\exp(k_1-1)]\bullet$$
$$[p_1 m_1^{t_1 k_2 + n_1} + p_2 m_2^{t_2 k_2 + n_2} + p_3 \sin(t_3 k_2 + n_3) + p_4] \tag{34}$$

Fig.7 shows the modified containment probabilities, in which the radius is determined through $k_m\sigma_{my}$. The maximum probability is 0.964 5 while the minimum 0.935 1, which means a reduced error containment with the mean of 0.950 3 much closer to 0.95. In addition, the standard deviation is 0.043 98 and the average absolute deviation 0.002 36, which implies a much better distribution and improved accuracy.

Therefore, the proposed method for improving EPU computation merits recommendation, in which EPU radius can be computed from Eq.(30), Eq.(31) and Eq.(34).

Furthermore, when k_2 is equal to zero, the extended

NACp model is tantamount to the traditional one which is appropriate to random error only. In this case, the containment probabilities of EPU radius can also be computed from Eq.(31). Thus the aforesaid NACp extended model and the calculation of EPU radius are of greater value in practices.
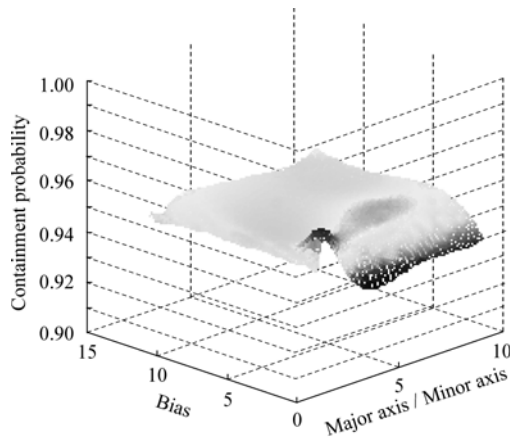

Fig.7   Containment probabilities of adjusting EPU radius.

4. Conclusions

The method to compute EPU through $k_{0.95}$ is convenient in modelling and simplifying analysis. This article proposes a revised method by using LSE for EPU radius calculation of random error based on the traditional NACp model and gains more accurate results than the existing method. Furthermore, this article puts forward an extended NACp model with biases considered and an approaching method to calculate EPU radius through $k_{0.95}$ by means of Taylor formula for the first time. Then a computation is carried out to transform $k_{0.95}$ to k_m for improving the accuracy. The EPU radius can be computed through $k_m \sigma_{my}$. Thus, NACp levels can finally be acquired in terms of codes by matching the EPU values to the specifications.

The estimation of $k_{0.95}$ is conservative, for it is based on the maximized $k_{0.95}$, i.e. k_m, which is larger than the truth less than 30%.

Some discussions are provided on two error models of NACp. Actually, some TIS-B systems have the function of pre-processing the source data and providing the corrected ones to users, thus facilitating them to calculate the accurate EPU radius using the output data. If the output data have not been corrected in TIS-B processing system or have residual biases, the EPU radius can be computed by the conservative equations presented in this article.

References

[1]   RTCA DO-289. Minimum aviation system performance standards for aircraft surveillance applications (ASA): appendix AC. Washington D. C.: RTCA Inc., 2003.

[2]   RTCA DO-242A. Minimum aviation system performance standards for automatic dependent surveillance broadcast (ADS-B). Washington D. C.: RTCA Inc., 2002.

[3]   RTCA DO-260A. Minimum operational performance standards for 1 090 MHz automatic dependent surveillance-broadcast (ADS-B) and traffic information service-broadcast (TIS-B). Washington D. C.: RTCA Inc., 2003.

[4]   Fu L, Fan Y Z, Ning W R. Investigation of tightly coupled SINS/GPS integration midcourse guidance for air-to-air missiles. Chinese Journal of Aeronautics 1998; 11(3): 206-213.

[5]   Huang J X, Wang Y D, Fan Y Z. Integrated GPS/INS of pseudo-range delta-range semi-physical simulations research. Chinese Journal of Aeronautics 1998; 11(4): 242-245.

[6]   Lou Y X. Analysis of radar accuracy. Beijing: National Defence Industry Press, 1979.

[7]   Chamlou R. TIS-B: calculation of navigation accuracy category for position and velocity parameters. IEEE Proceedings of The 23rd Digital Avionics Systems Conference. 2004; 1: 1.D.3-1-1.D.3-13.

[8]   Bourgeois R L, Castella F R. System integrity and track accuracy methodology for the traffic information service-broadcast (TIS-B). IEEE Proceedings of The 23rd Digital Avionics Systems Conference. 2004; 1: 1.B.3-1-1.B.3-10.

[9]   Ekstrand B. Tracking filters and models for seeker applications. IEEE Transactions on Aerospace and Electronic Systems 2001; 37(3): 965-977.

[10] Bazaraa N S, Shetty C M. Nonliner programming: theory and algorithms. New York: John Wiley and Sons, 1997.

Biography:

Zhang Qingzhu   Born in 1982, he received M.S. degree from School of Electronics and Information Engineering, Beijing University of Aeronautics and Astronautics. His main academic interests lie in automatic dependent service-broadcast, air traffic management and integrative information network.
E-mail: zhangqz_buaa@163.com